THE JOURNAL OF BIOLOGICAL CHEMISTRY VOL. 285, NO. 41, pp. 31304–31312, October 8, 2010

The Pih1-Tah1 Cochaperone Complex Inhibits Hsp90 Molecular Chaperone ATPase Activity*[S]

Received for publication, April 26, 2010, and in revised form, July 22, 2010 Published, JBC Papers in Press, July 27, 2010, DOI 10.1074/jbc.M110.138263

Kelvin Eckert[‡1,2], Jean-Michel Saliou[§1,3], Laura Monlezun[‡2], Armelle Vigouroux[‡], Noureddine Atmane[‡4], Christophe Caillat[‡5], Sophie Quevillon-Chéruel[¶], Karine Madiona[‡], Magali Nicaise[¶], Sylvie Lazereg[‖], Alain Van Dorsselaer[§], Sarah Sanglier-Cianférani[§], Philippe Meyer[‡4,6], and Solange Moréra[‡2,7]

From the [‡]Laboratoire d'Enzymologie et Biochimie Structurales (LEBS), CNRS, 91198 Gif-sur-Yvette, France, the [§]Laboratoire de Spectrométrie de Masse BioOrganique, Université de Strasbourg, IPHC, 25 rue Becquerel, 67087 Strasbourg, France, the [¶]Institut de Biochimie et de Biophysique Moléculaire et Cellulaire (IBBMC), CNRS, Université Paris-Sud, 91405 Orsay, France, and the [‖]Institut de Chimie des Substances Naturelles (ICSN), CNRS, 91198 Gif-sur-Yvette, France

Hsp90 (heat shock protein 90) is an ATP-dependent molecular chaperone regulated by collaborating proteins called cochaperones. This machinery is involved in the conformational activation of client proteins like signaling kinases, transcription factors, or ribonucleoproteins (RNP) such as telomerase. TPR (TetratricoPeptide Repeat)-containing protein associated with Hsp90 (Tah1) and protein interacting with Hsp90 (Pih1) have been identified in *Saccharomyces cerevisiae* as two Hsp90 cochaperones involved in chromatin remodeling complexes and small nucleolar RNP maturation. Tah1 possesses a minimal TPR domain and binds specifically to the Hsp90 C terminus, whereas Pih1 displays no homology to other protein motifs and has been involved in core RNP protein interaction. While Pih1 alone was unstable and was degraded from its N terminus, we showed that Pih1 and Tah1 form a stable heterodimeric complex that regulates Hsp90 ATPase activity. We used different biophysical approaches such as analytical ultracentrifugation, microcalorimetry, and noncovalent mass spectrometry to characterize the Pih1-Tah1 complex and its interaction with Hsp90. We showed that the Pih1-Tah1 heterodimer binds to Hsp90 with a similar affinity and the same stoichiometry as Tah1 alone. However, the Pih1-Tah1 complex antagonizes Tah1 activity on Hsp90 and inhibits the chaperone ATPase activity. We further identified the region within Pih1 responsible for interaction with Tah1 and inhibition of Hsp90, allowing us to suggest an interaction model for the Pih1-Tah1/Hsp90 complex. These results, together with previous reports, suggest a role for the Pih1-Tah1 cochaperone complex in the recruitment of client proteins such as core RNP proteins to Hsp90.

Heat shock proteins (Hsps)[8] or molecular chaperones were originally described as proteins with elevated expression levels under stress conditions such as a heat shock (1, 2). Many Hsps can act as complexes that correct the structures of misfolded or aggregated proteins (3, 4). Hsp90 is a particular molecular chaperone as the protein only binds to substrate proteins, which are in a late stage of folding and thus in a near-native conformation (5). Hsp90 is also essential for activating many signaling proteins such as kinases and hormone receptors in the eukaryotic cell under non-stress conditions (6, 7). Specificity toward such proteins (also called client proteins) is brought about by cochaperones, which interact with Hsp90 and regulate the chaperone cycle, leading to a complex containing Hsp90, the cochaperones, and the client protein (8, 9). Hsp90 functions as an ATP-dependent dimeric protein, which consists of three domains: a N-terminal domain (N) responsible for ATP binding, a middle domain (M) involved in cofactor/client binding and ATP hydrolysis, and a C-terminal domain (C) essential for dimerization, which is needed for Hsp90 activity (10). In this study, we worked with the Hsp90 homologue Hsp82, which is the stress-induced form in *Saccharomyces cerevisiae* (referred to as Hsp90 hereafter).

Yeast proteins Tah1 (111 residues, YCR060W) and Pih1 (344 residues, also named Nop17, YHR034C) have been identified as Hsp90-interacting cochaperones in three independent studies by two-hybrid screen or physical and genetic interaction screens (11–13). The C-terminal region of Tah1 (residues 75–11) has been shown to bind to Pih1 (14). So far, Pih1 is a protein of unknown function and may play a role in protein folding and/or rRNA processing by interacting with Hsp90, two chromatin-remodeling factors (Rvb1p, Rvb2p) and two rRNA-processing factors (Rrp43p, Nop58p) (11, 15). A protein similar to Pih1 has recently been identified in human (16) and homolog candidate molecules for Tah1 exist in *Drosophila* (termed Spaghetti, CG13570) and human (FLJ21908) as well (17). Whereas Tah1 contains a single TPR domain (TetratricoPeptide Repeat) with at least two TPR motifs (11), Pih1 has no known motifs. Pih1 alone is labile *in vivo* and *in vitro*, but is stabilized by Hsp90 together with Tah1 (14).

Numerous TPR domains have been characterized and structures are available in the Protein Data Bank. These domains are

* This work was funded by the CNRS, the Agence Nationale de la Recherche, the Association pour la Recherche sur le Cancer, the University of Strasbourg UdS, and the Region Alsace.

[S] The on-line version of this article (available at http://www.jbc.org) contains supplemental methods and Figs. S1 and S2.

[1] Both authors contributed equally to this work.

[2] Supported by a grant from the Agence Nationale pour la Recherche (ANR-05-JCJC No. 015101) (to S. M.).

[3] Supported by Sidaction.

[4] Supported by the Association pour la Recherche sur le Cancer.

[5] Supported by the Fondation pour la Recherche Médicale.

[6] To whom correspondence may be addressed. Tel.: 33-1-69-82-42-49; Fax: 33-1-69-82-31-29; E-mail: meyer@lebs.cnrs-gif.fr.

[7] To whom correspondence may be addressed. Tel.: 33-1-69-82-34-70; Fax: 33-1-69-82-31-29; E-mail: morera@lebs.cnrs-gif.fr.

[8] The abbreviations used are: Hsps, heat shock proteins; RNP, ribonucleoproteins; TPR, tetratricopeptide repeat; ITC, isothermal titration calorimetry.

responsible for protein-protein interactions. The TPR domains of Hsp90 cochaperones bind to the C-terminal residues EEVD of the Hsp90 as observed for Tah1 (18). Tah1 is specific for Hsp90 and binds as a monomer to the MEEVD motif of each Hsp90 subunit. Tah1 weakly stimulates the ATPase activity of Hsp90 (18). The latter activity coupled to conformational changes in Hsp90 and interactions with cochaperones facilitates activation of the Hsp90 diverse clientele.

To understand how Hsp90 acts on its clients, it is necessary to elucidate how cochaperones modify Hsp90 activity. Here, we present a biophysical and structural characterization of yeast Tah1 and Pih1 proteins, two Hsp90 cochaperones. These studies required large amounts of each protein. As Pih1 expression and stability seems to be puzzling (14), we developed a recombinant system based on multiple gene co-expression in *Escherichia coli* to produce a stable Pih1-Tah1 complex. A new multicistronic vector system (pKHS) that allows shuffling of multiple inserts by classic restriction and ligation techniques starting from a single set of vectors was employed to produce the Pih1-Tah1 complex at the milligram scale. Using a combination of biophysical techniques including analytical ultracentrifugation, microcalorimetry, and noncovalent mass spectrometry, binding stoichiometries, and oligomerization states of Tah1/Hsp90 and Pih1-Tah1/Hsp90 complexes were determined. A minimal interaction region between Pih1 and Tah1 was identified and the ability of the Pih1-Tah1 complex to regulate Hsp90 ATPase activity was investigated. Altogether our data allowed us to propose a protein interaction model for Pih1, Tah1, and Hsp90.

EXPERIMENTAL PROCEDURES

Vector pKHS Construction—The vector pKHS (kanamycin resistance) was constructed from the commercial pET28 expression plasmid (Novagen) (supplemental Fig. S1*A*). After XbaI and HindIII digestion, the extremities were blunted by the Klenow fragment and the vector was recircularized. The XbaI site is restored while the HindIII site is destroyed. The cloning cassette inserted into the NotI site was constructed with the primers: 5′-GGCCGCCCACCATCACCATCACCATTAGTGGAGCCACCCGCAGTTCGAAAAATAATT-3′ and 5′-GGCCAATTATTTTTCGAACTGCGGGTGGCTCCACTAATGGTGATGGTGATGGTGGGC-3′ and code for a six-histidine tag and the eight amino acids of the strep tag (19) separated by a suppressible stop codon. A unique NotI site is reconstituted in 5′ of the cassette and will be used for the cloning steps, while the NotI site in 3′ of the cassette is destroyed by insertion of an ORF.

Characteristics of the PCR Products—A single PCR product is synthesized for the cloning of a target gene in all of the positions in a polycistron. The restriction enzyme couple EagI and NotI is used for the preparation of all the different PCR products, with the possibility of replacing EagI with PspOMI or EaeI if necessary. The 5′ primer 5′-TTTTCGGCCGATTAATTTAAGAAGGAGATATATATATGNNNNNNNNNNNN-3′ used for the PCR amplification of all the genes encodes for a start codon followed by specific codons from the target gene. Upstream is an EagI restriction site (or PspOMI or EaeI sites) and a stop codon that is required for the upstream ORF in the polycistronic cloning. The rbs sequence of the pET series vector is positioned 8 base pairs before the start codon. The 3′ primer is simply composed of a coding sequence specific for the target gene followed by a NotI restriction site.

Cloning of tah1, pih1, and pih1-tah1 and Δpih1-tah1 into pKHS—The genes *pih1* and *tah1* were subcloned separately and together into the vector pKHS by introducing 3′ and 5′ EagI restriction sites by PCR as described above. The genes Δ*Pih1* (residues 1–185 were omitted) and *tah1* were subcloned together into pKHS. After restriction the resulting DNA fragments were ligated with the pre-cut vector. All further constructs were produced by EagI and NotI restriction of the appropriate inserts and recipient plasmids, respectively, followed by standard ligation procedures. One Shot MAX Efficiency DH5α-T1^R cells (Invitrogen) were transformed with the ligation mix according to the manufacturer's instructions. Cells containing plasmids were selected by plating on LB agar with kanamycin or ampicillin. The his tag (pKHS) is maintained in-frame with the last gene of the polycistron which is *tah1* in *pih1-tah1* and Δ*pih1(186–347)-tah1*. A cleavage site for TEV was added to the 3′-end of the gene Δ*pih1(186–347)-tah1* to eliminate the His_6 tag during purification leading to the presence of 8 additional residues.

Protein Production and Mass Determination by Gel Filtration—*E. coli* strains BL21 STAR (DE3) (Invitrogen) harboring the pKHS plasmids were used for co-expression and purification. Cells were grown at 37 °C in LB broth, containing the appropriate antibiotic, to an A_{600} of 0.8. Expression was then induced by addition of 0.5 mM IPTG, and growth continued for 4 h at 25 °C. Subsequently, cells were harvested, resuspended in buffer A (25 mM Tris pH 7.5, 10 mM imidazole, 300 mM NaCl) and disintegrated by sonication. Centrifugation at 50,000 × *g* for 1 h at 4 °C with subsequent filtration (Express PLUS 0.22 μm, Millipore) yielded cleared supernatant (cytosolic fraction). Cytosol was applied to a Ni-NTA-agarose column (10-ml bed volume). After washing with buffer A, buffer A supplemented with 300 mM imidazole was used for elution. Fractions containing the protein of interest were pooled and concentrated to 10 ml in a Vivaspin concentrator (Vivascience). Following gel-filtration chromatography separation on Superdex 75 or 200 26/60 column (GE Healthcare) equilibrated in 25 mM Tris buffer pH 7.5 containing 150 mM NaCl, protein containing fractions were pooled, concentrated as before, and stored at −80 °C. The His-tagged yeast Hsp90 and the Hsp90 MC (lacking the N-terminal domain) were purified as described previously (20). The typical yield was 8 mg of Tah1 and 13 mg of Pih1-Tah1 complex per liter of the corresponding culture.

Relative Molecular Mass (M_r) and Stokes Radius (Rs) Determination by Gel Filtration—Superdex 200 26/60 (GE Healthcare) gel-filtration chromatography was calibrated using the gel-filtration standards from GE Healthcare (aprotinin, M_r 6500; ribonuclease A, M_r 13,700, Rs 1.64 10^{-9} m; carbonic anhydrase, M_r 29,000, Rs 2.5 10^{-9} m; ovalbumin, M_r 43,000, Rs 3.05 10^{-9} m; conalbumin, M_r 75,000, Rs 4.04 10^{-9} m; aldolase, M_r 158,000, Rs 4.81 10^{-9} m; ferritin, M_r 444,000, Rs 6.1 10^{-9} m; thyroglobulin, M_r 669,000, Rs 8.5 10^{-9} m; blue dextran 2000; M_r 2,000,000). The relative molecular mass and Stokes radius

of Tah1 and Pih1-Tah1 were determined by logarithmic interpolation.

Matrix-assisted Laser Desorption/Ionization Time-of-flight Mass Spectrometry (MS) Analysis—Stained protein bands from the SDS-PAGE gel were excised and washed with 25 mM NH_4CO_3. In-gel tryptic digestion was performed following the standard protocol (21). Mass spectra were recorded in positive reflectron mode with a matrix-assisted laser desorption/ionization time-of-flight MALDI-TOF/TOF 4800 mass spectrometer (Applied Biosystem) using α-cyano-4-hydroxycinnamic acid (Sigma) as a matrix. Close calibration was performed using angiotensin I ($[M+H]^+$, 1296.68) and adrenocorticotropic hormone 18–39 ($[M+H]^+$, 2465.20). Mass tolerance was set to 15 ppm.

Analytical Ultracentrifugation: Sedimentation Velocity—Sedimentation velocity experiments with 86 μM Tah1 and 14 μM Pih1-Tah1 complex were carried using a Beckman Optima XLA ultracentrifuge equipped with an AN 60Ti four-hole rotor and cells with two-channel 12-mm path length centerpieces. Measurements were made at 40,000 rpm and 55,000 rpm for Pih1-Tah1 and Tah1, respectively, both at 15 °C. The Sednterp software was used to estimate the partial specific volumes from the amino acid composition of Tah1 (0.7244 $cm^3 \cdot g^{-1}$) and Pih1-Tah1 (0.7329 $cm^3 \cdot g^{-1}$) at 15 °C, as well the density (ρ = 1.00532 g/cm^3) and viscosity (η = 1.155 cP) of the buffer used. Sedimentation coefficient continuous c(S) distributions were determined using the Sedfit software (22).

Affinity and Stoichiometry Determination by ITC (Isothermal Titration Calorimetry)—The titration experiments were performed at 20 °C on a MicroCal ITC200 calorimeter (Northampton, MA) by injecting Hsp90 or Hsp90 MC with concentration ranging from 120 to 300 μM in the microcalorimeter cell (0.2 ml) containing Tah1 or Tah1-Pih1 with concentration ranging from 10 to 50 μM. 28 injections of 10 μl were performed at intervals of 180 s while stirring at 1000 rpm. The experimental data were fitted to a theoretical titration curve with software supplied by MicroCal (ORIGIN®). This software uses the relationship between the heat generated by each injection and ΔH (enthalpy change in $kcal \cdot mol^{-1}$), K_a (the association binding constant in M^{-1}), n (the number of binding sites), total protein concentration, and free and total ligand concentrations (23).

Noncovalent NanoESI-MS Experiments—Before mass spectrometry experiments, protein buffer was exchanged against 150 mM ammonium acetate buffer pH 7.5 using microcentrifuge gel-filtration columns (Zeba 0.5 ml, Thermo Scientific, Rockford, IL). Protein concentrations were determined spectrophotometrically.

Mass spectrometry experiments were performed on two instruments operating in the positive ion mode. An electrospray time-of-flight mass spectrometer (LCT, Waters, Manchester, UK) equipped with an automated chip-based nanoESI source (Triversa Nanomate, Advion Biosciences, Ithaca, NY) was used to analyze the Pih1-Tah1 and ΔPih1-Tah1 complexes and the titration of Hsp90 with these two complexes. A hybrid quadrupole/ion mobility separator/time-of-flight instrument (Synapt HDMS, Waters, Manchester, UK) was used to perform titration of Hsp90 with Tah1. In this case samples were loaded into 4-μm i.d. PicoTip nanospray emitters (New Objective, Woburn, MA) and directly infused. External calibration was performed with the multiply charged ions produced by 2 μM horse heart myoglobin diluted in 1:1 (v/v) water/acetonitrile acidified with 1% (v/v) formic acid or using the singly charged ions produced by a 3 mg/ml solution of caesium iodide in 2-propanol/water (1/1). Mass measurements under denaturing conditions were carried out by diluting samples to 2 μM in water/acetonitrile/formic acid (50:50:1) with Vc = 40 V and P_i = 1.1 mbar.

Experiments under nondenaturing conditions were realized in 150 mM ammonium acetate buffer at pH 7.5. Optimal accelerating voltages were applied to the sample cone (Vc) and a well-adapted pressure in the interface (P_i) was used. This allowed the fragile noncovalent assemblies to be transferred from the solution to the gas phase while remaining intact and at the same time achieved efficient ion desolvation and ion transmission through the mass spectrometer (24). P_i and Vc values are reported in figures legends. Data analysis and MaxEnt 1 deconvoluted spectra were performed with MassLynx 3.5 (Waters, Manchester, UK).

Hsp90 ATPase Activity Assays—The Hsp90 ATPase activity assays were performed as previously described (25), with slightly modified conditions using 50 mM Tris-HCl buffer pH 7.5, KCl 50 mM and 3 mM $MgCl_2$. To avoid Pih1-Tah1 precipitation the experiments were carried out at 25 °C on a UVIKON XS spectrophotometer. Hsp90 activity measurements were carried out using 5 μM Hsp90 and background ATPase activity was determined by the addition of 15 μM of geldanamycin (Sigma). Hsp70 (Stressgen) ATPase activity measurements were carried out using 2 μM enzyme, and background activity was determined before Hsp70 addition (26). The cochaperones Pih1-Tah1, ΔPih1-Tah1, and Tah1, as well as the AGT-gp45 control complex (27) were added as indicated. All measurements were repeated three to six times.

RESULTS

Tah1, Pih1, and Pih1-Tah1 Protein Complex Expression using the pKHS Vector—The pKHS system uses a single pair of restriction enzymes common for all the genes to be cloned along the polycistron (see supplemental methods and Fig. S1). Two constructs for the expression of yeast *pih1(1–344)* and *tah1(1–111)* were realized as well as the two bicistrons *pih1-tah1* and Δ*pih1(186–344)-tah1*. All these constructs were efficiently expressed in *E. coli* host cells. The pKHS His-tagged yeast Pih1 (called Pih1-His_6 throughout the text) is a protein of 353 residues. The His-tagged yeast Tah1 (called Tah1 throughout the text) consists of 119 amino acids. The yeast pKHS Pih1-Tah1 complex bearing a histidine tag on Tah1 (named Pih1-Tah1 throughout the text) is composed of 347 and 119 residues for Pih1 and Tah1 respectively. Finally, the truncated yeast Pih1(186–344)-Tah1 complex (named ΔPih1-Tah1 throughout the text) obtained after the His-tag cleavage of Tah1 is formed by 161 and 118 residues for ΔPih1 and Tah1, respectively. The expected masses of each protein or complex are summarized in Table 1.

Pih1 Is Highly Degraded in Its N-terminal Region—SDS-PAGE analysis of the purified Pih1-His_6 (Fig. 1*A*) showed the presence of four main bands that were further submitted to protein identification by MALDI-TOF peptide mass finger-

printing. The upper band (band 1) at ~40 kDa corresponds to full-length Pih1-His_6. Bands 2 and 3 that migrate at ~19 kDa and band 4 with an apparent molecular mass of 13 kDa were attributed to Pih1-His_6 degradation products. The identified sequence covers a C-terminal region of Pih1-His_6 starting from either residue 189 (bands 2 and 3) or residue 234 (band 4). After concentration and storage at −80 °C, the same Pih1-His_6 was also analyzed by electrospray ionization mass spectrometry (ESI-MS) in classical denaturing conditions (Fig. 1*B*). Two species were detected: a minor species at 19,151.6 ± 0.3 Da, which corresponds to the truncated 186-Cter Pih1-His_6 (theoretical molecular mass, 19,151.6 Da) probably related to band 2 in Fig. 1*A* and a major species at 17,670.0 ± 0.4 Da corresponding to an even shorter form of Pih1-His_6 (199-Cter, see band 3 in Fig. 1*A*). No full-length protein was then detected by ESI-MS, probably due to its low stability.

Tah1 Is Stable and Monomeric—The purified Tah1 had an apparent molecular mass of 13 kDa by SDS-PAGE close to its calculated mass (data not shown). On gel filtration, Tah1 migrated as a single peak corresponding to a protein with a Stokes radius of 1.83 10^{-9} m and an apparent mass of 16 kDa, assuming a globular protein. Data from sedimentation velocity analysis conducted on Tah1 showed a single species with a sedimentation coefficient $S_{20,w}$ of 1.57 S (Table 2). This value is in agreement with that of a monomer presenting a calculated frictional ratio value (f/f_0) of 1.33 (f/f_0 is 1.25 for a globular protein (28)) and a calculated Stokes radius of 2.08 10^{-9} m close to that evaluated by gel filtration. Analysis of the diffusion coefficient leading to an apparent molecular mass of 13 kDa also demonstrated that Tah1 is monomeric. Finally, to unambiguously determine Tah1 oligomerization state, noncovalent mass spectrometry experiments were conducted and revealed that Tah1 was present as a monomer with a measured molecular mass of 13,416 ± 1 Da (expected mass of the full-length Tah1 with deletion of the N-terminal methionine residue is 13,416 Da, Fig. 2 and Table 3). Altogether these results obtained from a panel of biophysical techniques led us to the conclusion that Tah1 is present in a rather elongated monomeric form, which is common for TRP-domain proteins (29).

TABLE 1
Measured molecular weights in denaturing conditions

Protein or Complex analyzed	Name	Symbol	Expected Mass (Da)	Measured Mass in denaturating conditions (Da)	Sequence detail
Pih1-His_6	Pih1-His_6		40 555.4	ND	Pih1(1-344)-AAAHHHHHH
	ΔPih1	◇	19 151.6	19 151.6 ± 0.3	Pih1(**186**-344)-AAAHHHHHH [(a)]
	$Pih1_{mini}$	▽	17 669.9	17 670.0 ± 0.4	Pih1(**199**-344)-AAAHHHHHH [(a)]
Tah1	Tah1	○	13 416.0	13 416.1 ± 0.2	Tah1(**2**-111)-AAAHHHHHH
Pih1-Tah1 complex	Pih1	□	39 645.4	39 645.8 ± 0.4	Pih1(**2**-344)-AAD
	Tah1	○	13 416.0	13 416.0 ± 0.1	Tah1(**2**-111)-AAAHHHHHH
ΔPih1-Tah1 complex	ΔPih1	◇	18 372.8	18 372.5 ± 0.1	Pih1(**186**-344)-AAD
	$Pih1_{mini}$	▽	16 891.1	16 891.6 ± 0.4	Pih1(**199**-344)-AAD [(b)]
	Tah1	○	13 318.9	13 319.3 ± 0.4	Tah1(**2**-111)-SGENLYFQ
Hsp90	Hsp90	0	82 718.7	82 723.6 ± 1.7	MRGSHHHHHHG-Hsp90(1-709)
	$Hsp90_{gluco}$		82 896.7	82 903.1 ± 2.5	MRGSHHHHHHG-Hsp90(1-709) [(c)]

ND, not detected.
[(a)] Degradation product of Pih1(1–344)-AAAHHHHHH.
[(b)] Degradation product of Pih1(186–344)-AAD.
[(c)] Gluconoylation of MRGSHHHHHH-Hsp90(1–709) (45).

Pih1-Tah1 Forms a 1:1 Heterodimer—Gel filtration of the purified Pih1-Tah1 complex (expected mass of ~53 kDa for a 1:1 complex) yielded three peaks corresponding to apparent molecular masses of 100, 52, and 16 kDa (Fig. 3*A*). When analyzed by SDS-PAGE the first peak showed two bands corresponding to Pih1 (~40 kDa) and Tah1 (~13 kDa); the second peak contained multiple low molecular mass bands and the third, only one band around 13 kDa (Fig. 3*B*). We turned to MALDI-TOF peptide mass fingerprinting analysis for protein identification. As expected full-length Pih1 and Tah1 were identified in the first gel filtration peak, while the third peak only contained Tah1. In the second gel filtration peak, Tah1 was identified in the 13 kDa region while the other low molecular mass bands could be assigned to Pih1 degradation products as similarly observed for Pih1 purification. Again, the sequence coverage of degraded Pih1 ranged at least from residue 186 to the C terminus. Further ESI-MS experiments performed on the first gel filtration peak in denaturing conditions confirmed the presence of the two full-length proteins Tah1 (13,416.0 ± 0.1 Da) and Pih1 (39,645.8 ± 0.4 Da) devoid of their N-terminal methionine residue (see Table 1).

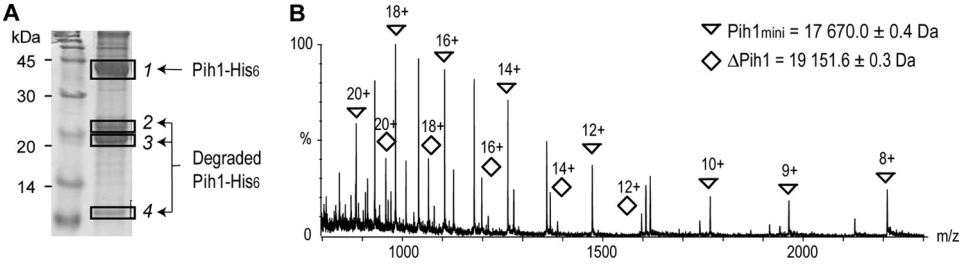

FIGURE 1. **Purification of Pih1.** *A*, purified samples from the gel filtration were analyzed on a 18% SDS-PAGE. Protein bands were identified by MALDI-TOF peptide mass fingerprinting. *B*, nanoESI-MS analysis in denaturing conditions of Pih1-His_6 (8 μM).

The stoichiometry of the Pih1-Tah1 complex (gel filtration peak 1) was first investigated by analytical ultracentrifugation using sedimentation velocity. The sedimentation coefficient distribution revealed the presence of a single species with a $S_{20,w}$ of 3.2 S (Table 2). This value is compatible with a complex consis-

TABLE 2
Sedimentation characteristics of Tah1 and Pih1-Tah1 complex
GF is for gel filtration. $S_{20,w}$ is the sedimentation coefficient, f and f_0 are the friction coefficients and R_S is the Stokes radius.

Protein and concentration	MW by MS	MW by GF	*Rs* by GF	$S_{20,w}$ value[a]	f/f_0	R_s
μM	*Da*	*Da*	*m*	$cm^3 \cdot g^{-1}$		*m*
Tah1 (86)	13,416	16,000	1.83×10^{-9}	1.57	1.33	2.08×10^{-9}
Pih1-Tah1 (14)	39,645.4 13,416	100,000	4.3×10^{-9}	3.2	1.57	3.91×10^{-9}

[a] The detected species were determined by sedimentation coefficient distribution c(S) analysis of the radial distributions using the Sedfit software (22).

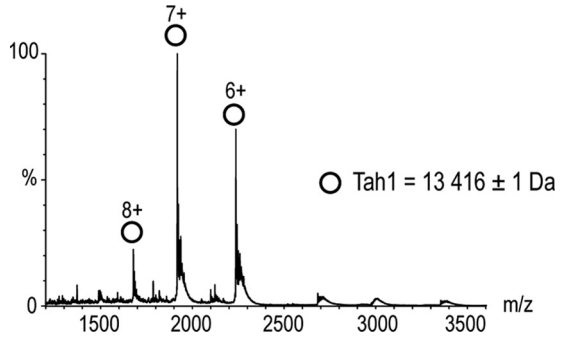

FIGURE 2. **Determination of Tah1 oligomeric state by noncovalent MS.** NanoESI mass spectra were obtained under nondenaturing conditions for Tah1 (8 μM). (Vc = 140 V; P_i = 4 mbar).

TABLE 3

Measured molecular weights in noncovalent conditions

Discrepancies between measured and theoretical MWs in nondenaturing conditions can be explained by: (i) Hsp90 heterogeneity as observed in denaturing conditions (see Table 1) and (ii) less efficient desolvation of Hsp90 high MW complex in the mass spectrometer leading to peak broadening and less precise mass measurements.

Protein or Complex analyzed	Symbol	Expected Mass (Da)	Measured Mass in noncovalent conditions (Da)	Precision (%)	Binding Stoichiometries	Figure
Tah1	○	13 416	13 416 ± 1	< 0.01	monomer Tah1	2
Pih1-Tah1 complex	□○	53 061	53 065 ± 4	< 0.01	1 :1 Pih1-Tah1	3C
ΔPih1-Tah1 complex	◇○	31 691	31 695 ± 2	0.01	1:1 ΔPih1-Tah1	4
	⧖○	30 210	30 211 ± 1	< 0.01	1:1 $Pih1_{mini}$-Tah1	
Hsp90/Tah1 complex	○○	165 437	166 092 ± 36	0.40 *	dimer $(Hsp90)_2$	5A
	○○○	178 853	179 556 ± 31	0.40 *	$(Hsp90)_2$/ Tah1	
	○○○○	192 269	193 175 ± 45	0.47 *	$(Hsp90)_2$/ $(Tah1)_2$	
Hsp90/Pih1-Tah1 complex	○○	165 437	166 022 ± 19	0.35 *	dimer $(Hsp90)_2$	5B
	□○○	218 498	219 193 ± 38	0.32 *	$(Hsp90)_2$ / Pih1-Tah1	
	□□○○	271 560	272 353 ± 38	0.29 *	$(Hsp90)_2$ / $(Pih1\text{-}Tah1)_2$	

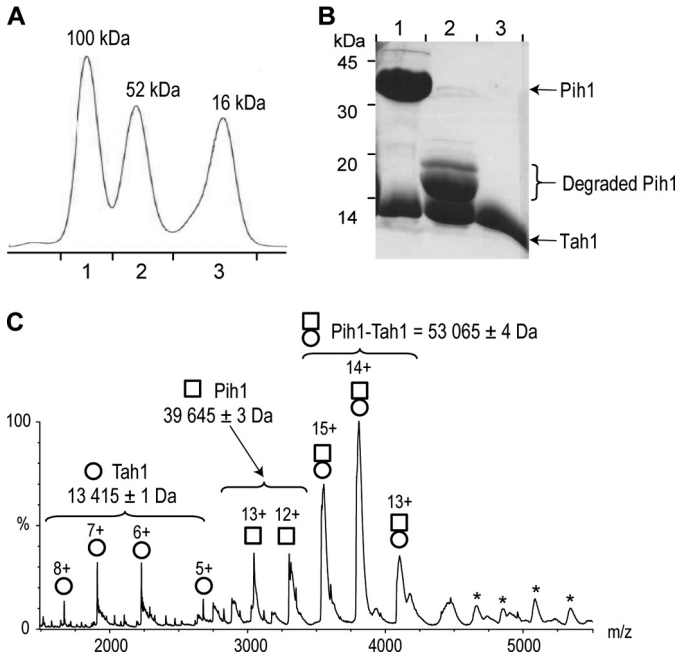

FIGURE 3. **Co-purification and stoichiometry of the Pih1-Tah1 complex.** *A*, gel filtration profile showing three elution peaks. *B*, 12% SDS-PAGE of gel filtration elution peaks. Lane numbers correspond to the peak numbers in *panel A*. Protein bands were identified by MALDI-TOF peptide mass fingerprinting. *C*, noncovalent mass spectrometry analysis of the Pih1-Tah1 complex (first peak of the gel filtration in *panel A*). NanoESI mass spectra were obtained under nondenaturing conditions for Pih1-Tah1 (8 μM) (Vc = 120 V; P_i = 7 mbar). * represents the very minor ion series of $(Pih1\text{-}Tah1)_2$.

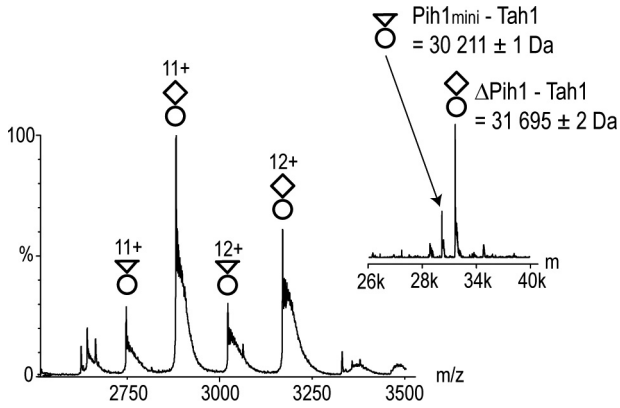

FIGURE 4. **Determination of the ΔPih1-Tah1 binding stoichiometry by noncovalent MS.** NanoESI mass spectra were obtained under nondenaturing conditions for ΔPih1-Tah1 (24 μM) (Vc = 120 V; P_i = 7 mbar). *Insets* correspond to deconvoluted ESI mass spectra.

ting of one Pih1 and one Tah1 molecule presenting a calculated frictional ratio value (f/f_0) of 1.57 and a calculated Stokes radius of 3.9 10^{-9} m which is close to the Stokes radius of 4.3 10^{-9} m evaluated by gel filtration and corresponding to a 100 kDa globular protein. Therefore, the complex behaved as a homogeneous elongated form which explains its high apparent molecular mass found in gel filtration. The binding stoichiometry of the Pih1-Tah1 complex was also investigated by noncovalent mass spectrometry. ESI mass spectra confirmed the presence of a 1:1 Pih1:Tah1 complex with a measured molecular mass of 53,065 ± 4 Da (expected mass of the complex 53 061 Da) in addition to the free Tah1 (13,415 ± 1 Da) and Pih1 (39,645 ± 3 Da) proteins (Fig. 3*C* and Table 3).

Determination of a Minimal Pih1 Region Necessary for the Formation of a 1:1 Pih1-Tah1 Complex—ESI-MS under denaturing conditions showed that the purified Pih1-His_6 degrades into two main C-terminal products beginning either from residue 186 or 199. The MALDI-TOF peptide mass fingerprinting analysis revealed a similar Pih1 degradation product (186-Cter), which co-elutes with Tah1 and which is thus responsible for interaction with Tah1. After the identification of this minimal Tah1 binding region within Pih1 (186-Cter), called ΔPih1, we cloned Δ*Pih1-tah1* into the pKHS vector and co-purified this truncated complex in which the His_6 tag on Tah1 was cleaved. The unique gel filtration peak was analyzed by ESI-MS under denaturing conditions (data not shown) and confirmed the presence of the full-length protein Tah1 without its N-terminal methionine residue and with 8 additional residues at the C terminus (13,319.3 ± 0.4 Da, expected 13,318.9 Da) and the truncated form of Pih1 (18,372.5 ± 0.1 Da, expected 18,372.8 Da)

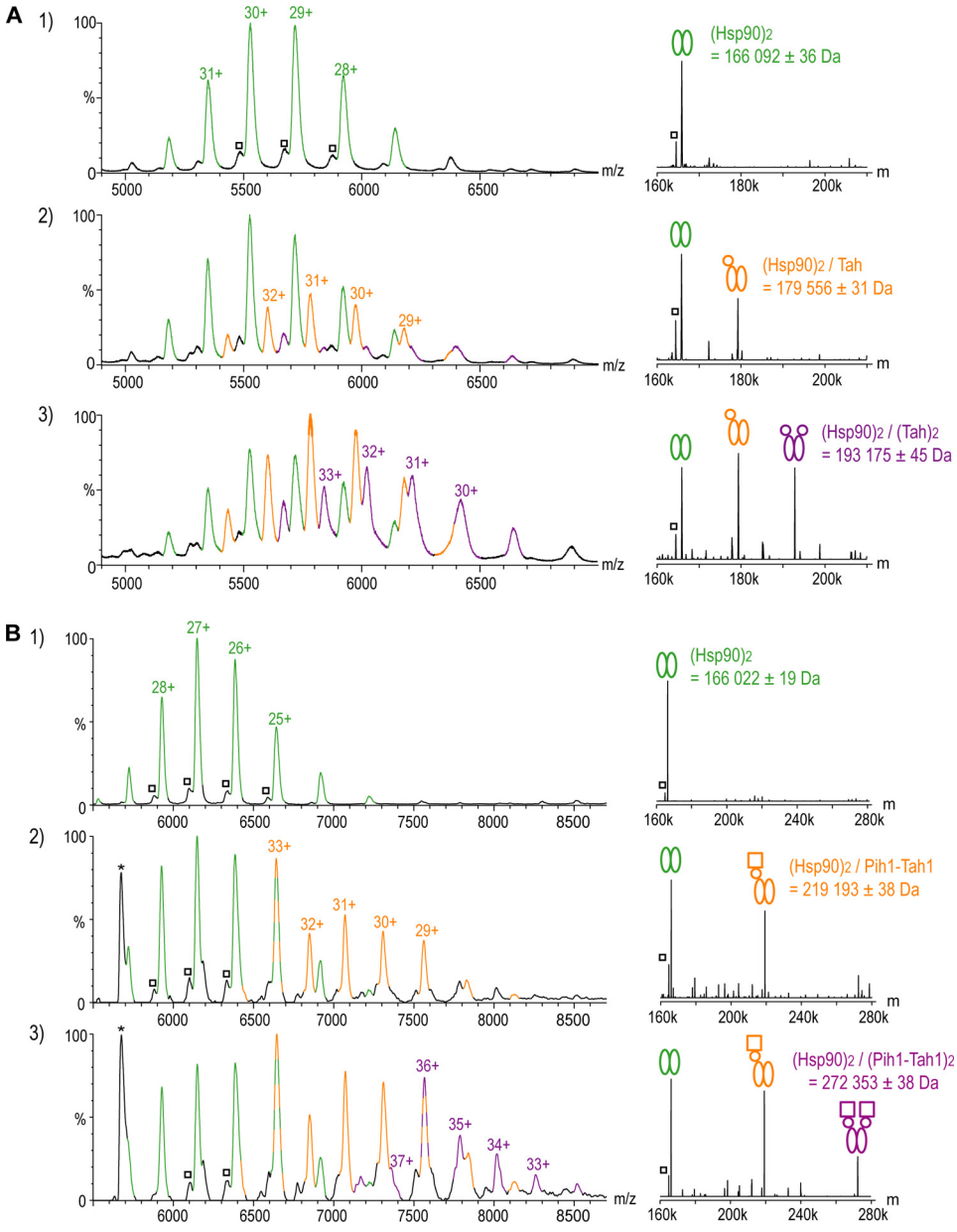

FIGURE 5. **Determination of Tah1/Hsp90 and Pih1-Tah1/Hsp90 binding stoichiometries by noncovalent MS.** *A*, nanoESI mass spectra were obtained under nondenaturing conditions for Hsp90 (4 μM) alone (*1*) and in the presence of 8 μM Tah1 (*2*) or 16 μM Tah1 (*3*) (Vc = 180 V; P_i = 6.5 mbar). *Insets* correspond to deconvoluted ESI mass spectra. *B*, nanoESI mass spectra were obtained under nondenaturing conditions for Hsp90 (4 μM) alone (*1*) and in the presence of 4 μM Pih1-Tah1 (*2*) or 8 μM Pih1-Tah1 (*3*) (Vc = 180 V; P_i = 7 mbar). * corresponds to Pih1 signal and □ to slight fragmentation of Hsp90 dimer because of the high Vc value necessary for ion transmission of complexes. Peaks resulting from two species are *bicolored*. *Insets* correspond to deconvoluted ESI mass spectra.

Determination of Tah1/Hsp90 and Pih1-Tah1/Hsp90 Binding Stoichiometries—Previously published ITC experiments showed that Hsp90 binds Tah1 in a 1:1 ratio (a monomer of Tah1 for a monomer of Hsp90) (18). To validate the Tah1/Hsp90 stoichiometry and to determine the stoichiometry of the Pih1-Tah1/Hsp90 complex, noncovalent mass spectrometry was employed. Hsp90 was analyzed alone and with increasing concentrations of either Tah1 or Pih1-Tah1 (Fig. 5, *A* and *B*, respectively and Table 3). In absence of any binding protein partner, Hsp90 is detected as a dimer (166,092 ± 36 Da and 166,022 ± 19 Da, expected 165,437 Da, Fig. 5, *A* and *B*, *panel 1* and Table 3). When increasing amounts of Tah1 are added, an ion series corresponding to a 1:2 Tah1:Hsp90 complex first appears (179,556 ± 31 Da, expected 178,853 Da, Fig. 5*A*, *panel 2* and Table 3). With a 4-fold Tah1 excess, the equilibrium is displaced toward the formation of a 2:2 Tah1:Hsp90 (193,175 ± 45 Da expected 192,269 Da, Fig. 5*A*, *panel 3* and Table 3), which is in agreement with results obtained from microcalorimetry analysis (18).

Similarly, in the presence of increasing amounts of Pih1-Tah1 complex, species corresponding to 1:1:2 (219,193 ± 38 Da, expected 218,498 Da) and 2:2:2 Pih1-Tah1/Hsp90 (272,353 ± 38 Da, expected 271,560 Da) ternary complexes were observed (Fig. 5*B*, *panels 2* and *3* and Table 3). Therefore a Pih1-Tah1 heterodimer can bind to a monomer of Hsp90. The same results were obtained with the truncated ΔPih1-Tah1 in the presence of Hsp90 (see supplemental Fig. S2). Four ternary complexes were observed: 1:1:2 and 2:2:2 for ΔPih1-Tah1/Hsp90 and $Pih1_{mini}$-Tah1/Hsp90 assemblies.

(Table 1). Interestingly, a shorter form of Pih1 with a molecular mass of 16,891.6 ± 0.4 Da was also identified. This corresponds to the shorter fragment of degraded purified Pih1 (199-C-ter) now called $Pih1_{mini}$ (expected 16,891.1 Da) (Table 1). Notably, this fragment seems to be stable and still interacts with Tah1, as deduced from noncovalent MS analysis of the ΔPih1-Tah1 preparation where both 1:1 ΔPih1:Tah1 (31,695 ± 2 Da, expected 31 691 Da) and 1:1 $Pih1_{mini}$:Tah1 (30,211 ± 1 Da, expected 30,210 Da) were detected (Fig. 4 and Table 3). Therefore, the region from amino acid 199 to the C terminus of Pih1 is still sufficient for Tah1 binding.

Thermodynamics of the Interactions between Tah1 or Pih1-Tah1 and Hsp90 at 20 °C—The dissociation constant (K_d) and the stoichiometry (N) values between Tah1 or Pih1-Tah1 and Hsp90 were determined using isothermal titration calorimetry (Fig. 6). The mean K_d values were similar, 1.3 μM for Tah1 and 1.6 μM for Pih1-Tah1. The micromolar range observed here is in line with the values found for other Hsp90 cochaperones (18, 30–33). The determined stoichiometry was close to one for both Pih1-Tah1 and Tah1, implying that a monomer of Tah1 or

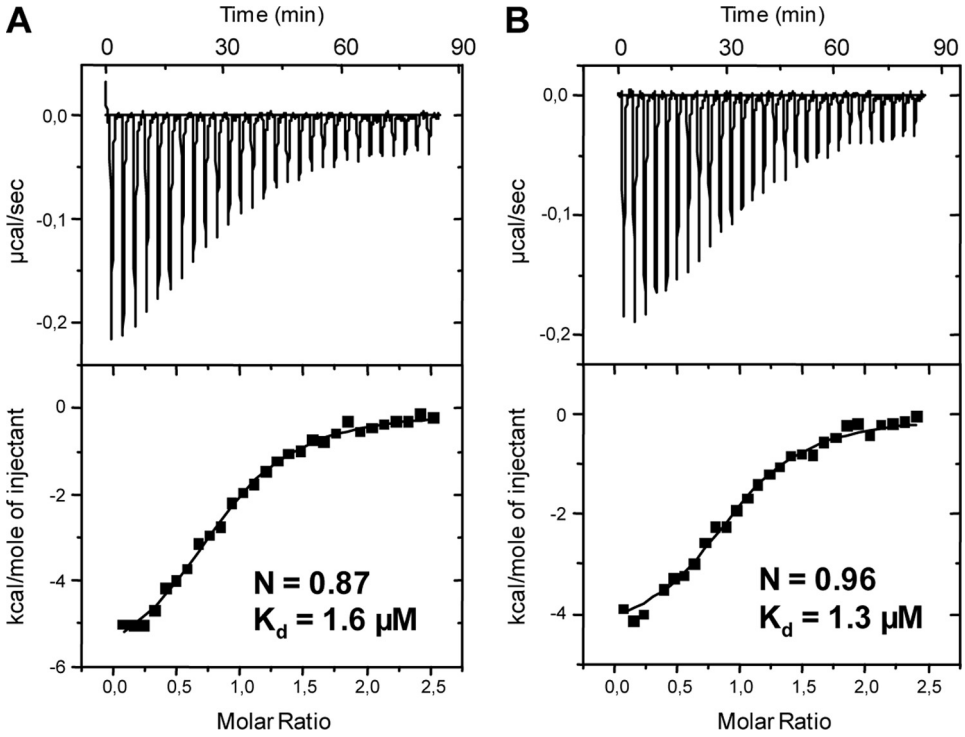

FIGURE 6. **ITC of Tah1 and Pih1-Tah1 complex binding to Hsp90.** ITC data obtained by injecting Hsp90 into *A*, Tah1 and *B*, Pih1-Tah1. *Lower panels* show the fit to the binding curve with the resulting affinities (K_d) and stoichiometries (*N*). Both Tah1 and Pih1-Tah1 bind Hsp90 with similar affinities (K_d of 1.6 μM and 1.3 μM, respectively).

a heterodimer of Pih1-Tah1 can bind to a monomer of Hsp90. Both the Pih1-Tah1 complex and Tah1 also displayed significant affinity toward Hsp90 MC, which lacks the N-terminal domain and the linker region (data not shown) confirming that the C-terminal moiety of Hsp90 is responsible for Tah1 and Pih1-Tah1 binding.

Regulation of Hsp90 ATPase Activity—We tested weather the Pih1-Tah1 complex could regulate the ATPase activity of Hsp90 and we observed that in the concentration range used, Pih1-Tah1 inhibited the ATPase activity of 5 μM Hsp90 in a concentration-dependent manner, reaching ~25% inhibition at 20 μM (Fig. 7*A*). Further concentrated Pih1-Tah1 complex could not be used in the assay, as it tended to precipitate and interfered with the measurement. An unrelated control protein complex failed to inhibit the Hsp90 ATPase (Fig. 7*C*), whereas the Pih1-Tah1 complex had no effect on the activity of the Hsp70 chaperone (Fig. 7*D*), showing that the observed inhibition was specific. Pih1 appeared responsible for this inhibition as Tah1 alone weakly stimulated the ATPase activity of Hsp90 as previously described (18) and confirmed here (Fig. 7*B*). The ΔPih1-Tah1 complex formed with a N-terminal-truncated Pih1 was also an inhibitor of Hsp90 ATPase activity although to a lower extent (Fig. 7*B*).

DISCUSSION

Hsp90 action on client proteins takes place within dynamic multiprotein complexes with a variety of cochaperones whose biological roles in client activation and chaperone machinery regulation remain largely unexplored. Furthermore, as new Hsp90 client proteins are discovered the number of cochaperones tends to grow as well. Some of these cochaperones appear to regulate specifically the Hsp90-client protein interaction. To characterize the role of the Pih1 and Tah1 cochaperones, we developed a polycistronic expression system (pKHS) to overcome inherent Pih1 instability and we successfully produced a stable Pih1-Tah1 complex. We were thus able to examine the interaction and action of both Tah1 and the Pih1-Tah1 complex on Hsp90. Analytical ultracentrifugation, microcalorimetry, and noncovalent mass spectrometry were all in agreement in the determination of the Pih1 and Tah1 oligomerization state and binding stoichiometry to Hsp90. Tah1 is a monomeric cochaperone and forms a heterodimeric complex with Pih1 with a 1:1 stoichiometry. Both Tah1 and Pih1-Tah1 can bind to a subunit of Hsp90 as previously observed for Tah1 (18) thus two Tah1-Pih1 cochaperone heterodimers can bind to a dimer of Hsp90. A 1:1:2 Pih1-Tah1/Hsp90 complex was also observed in noncovalent MS experiment. Because Hsp90 expression level is generally much higher than that of its cochaperone (34), asymmetric binding of one Pih1-Tah1 heterodimer per Hsp90 dimer cannot be ruled out. Such an asymmetry has been observed for the cochaperone Aha1 that binds preferentially as a monomer *in vivo* (35). Interestingly, Pih1 alone and in complex with Tah1 undergoes a similar degradation of its N-terminal region during its purification. This allowed us to map the protein interaction region of Pih1 to Tah1. Based on previous work by Zhao *et al.* (14) and on our new data, we can propose a putative protein interaction model for Pih1, Tah1, and Hsp90 (Fig. 8). The Tah1-C-terminal region (residues 76–111) and $Pih1_{mini}$ (residues 199–344) are sufficient to interact with each other. As the C-terminal region of Tah1 in addition to its TRP domain are required for interaction with the C-terminal domain of Hsp90 (14), binding of Pih1 to Tah1 positions the C-terminal domain of the three proteins in close vicinity to each other (Fig. 8).

We also investigated the ability of Pih1-Tah1 to regulate the Hsp90 ATPase activity. Tah1 was previously shown to induce a slight stimulation on Hsp90 (18). Although this stimulation was confirmed in our study, we showed that the addition of the Pih1-Tah1 complex resulted in the inhibition of Hsp90 ATPase. Furthermore, the ΔPih1-Tah1 complex conserves the ability to inhibit Hsp90 indicating that the C-terminal moiety of Pih1 is sufficient for this activity. This inhibition reached ~25% at 20 μM of the cochaperone complex, corresponding in our assay to 4× molar excess of Pih1-Tah1 over Hsp90. We cannot rule out a dissociation of the Pih1-Tah1 complex upon its dilution during the measurement that could result in lower inhibi-

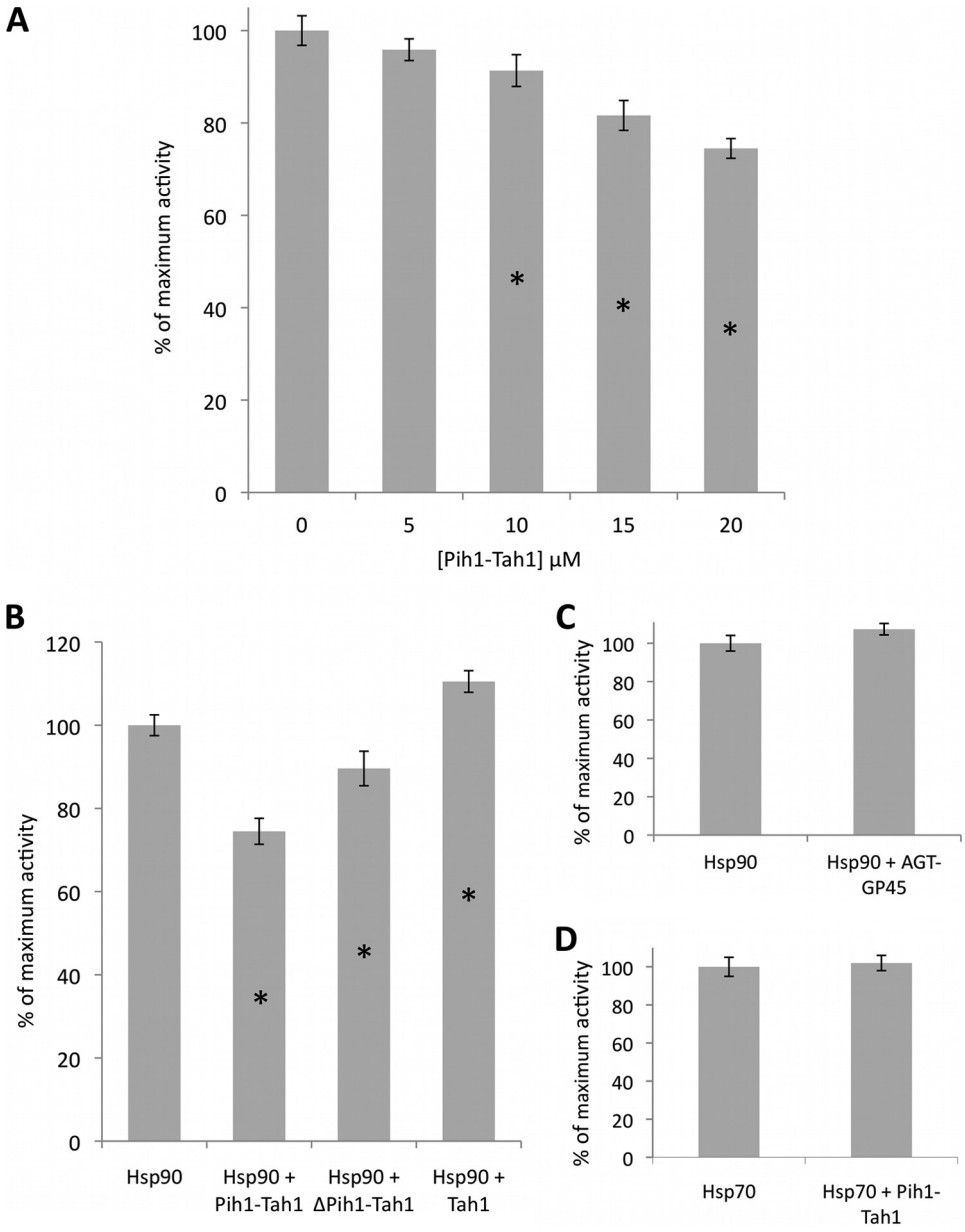

FIGURE 7. **Antagonist effect of Pih1-Tah1 and Tah1 on Hsp90 ATPase activity.** *A*, ATPase activity of 5 μM Hsp90 in the presence of an increasing amount of the Pih1-Tah1 complex. *B*, differential effect of 20 μM of Pih1-Tah1, ΔPih1-Tah1, or Tah1 on the ATPase activity of 5 μM Hsp90. *C*, effect of 20 μM of the unrelated AGT-gp45 complex on the ATPase activity of 5 μM Hsp90. *D*, effect of 20 μM of Pih1-Tah1 complex on the ATPase activity of 2 μM Hsp70. Data are averages of three to six repeated measurements, and error bars refer to standard deviations. * indicates statistical significance of the difference between the average of that experiment with the average of the control in absence of cochaperones as assessed by a *t* test ($p < 0.05$).

tion rates, since Tah1 alone activates Hsp90 ATPase. However, similar Hsp90 inhibition rates were observed for the kinase specific yeast cochaperone Cdc37 where ~30 μM of cochaperone was needed to exert ~20% inhibition (31).

Our data demonstrated that both Pih1-Tah1 and Tah1 displayed similar affinity toward Hsp90 suggesting that Pih1-Hsp90 interaction is likely very weak in line with the pull-down assays showing no significant binding between both purified Hsp90 and Pih1 (14). Therefore, we propose that Tah1 serves as a primary anchor to Hsp90 while Pih1 binding is involved in the ATPase down-regulation. Indeed, addition of a large excess of the Hsp90 C-terminal nine residues peptide (ADTEMEEVD), containing the Tah1 TPR-domain binding motif, in the Hsp90 inhibition assay partially rescue Hsp90 basal activity (data not shown), indicating that Tah1 binding is essential for the Pih1-Tah1 activity on Hsp90.

ATP hydrolysis was shown to trigger client protein release from Hsp90 (36) and cochaperones that inhibit Hsp90 ATPase such as Cdc37 and Sti1/Hop are thought to facilitate client loading onto Hsp90 (31, 37). The mechanism of this coupled client loading and ATPase inhibition has been best characterized for the cochaperone Cdc37 that specifically recruits the kinase clients to Hsp90 (38). Together with the results obtained for Sti1/Hop (39–41), it suggests a general mechanism for client loading where the cochaperone recruits the client and at the same time blocks the progression through the Hsp90 ATPase cycle, maintaining its dimeric clamp in an open conformation likely to favor client binding. Indeed, the localization of the Pih1-Tah1 bound to Hsp90 C-terminal moiety could lock the hinge region situated between the middle and C-terminal region of Hsp90 (Ref. 20 and Fig. 8) and keep Hsp90 in an opened conformation preventing the N-terminal domain dimerization necessary for the ATPase activity.

The Hsp90 machinery is implicated in the L7ae RNP assembly. Hsp90 inhibition by geldanamycin results in decreased levels of newly synthesized RNPs (U4, telomerase, etc) and in loss of several core RNP proteins such as 15.5K and Nop58 (17). The cochaperone Pih1 can also directly interact with these core proteins (14, 15, 17, 42). These observations together with our finding of the inhibitory effect of the Pih1-Tah1 complex on Hsp90 ATPase, which is thought to facilitate client binding, suggest that the Pih1-Tah1 cochaperone could act as a platform for the recruitment and loading of client proteins involved in RNP assembly onto the Hsp90 chaperone.

The RuvB-like proteins Rvb1 and Rvb2 have been shown to associate with Pih1 and Tah1 in the so-called R2TP complex (11). Because Rvb1 and Rvb2 have similarities with AAA+ helicases and present coupled ATPase and unwinding activities (43) it is tempting to imagine that Rvb1/Rvb2 could cooperate with the Hsp90-Tah1-Pih1 machinery and act on the remodel-

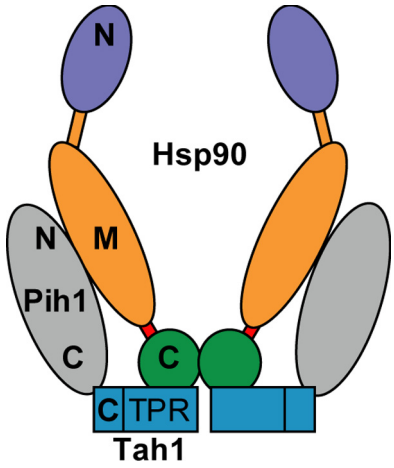

FIGURE 8. **A protein interaction model for Pih1, Tah1, and Hsp90.** Tah1 binds the C-terminal domain of Hsp90 (*C*, *green*) through its TPR domain (TPR, *blue*) and the Pih1 C-terminal domain (Pih1 C, *gray*) through its C-terminal part. To explain the observed Hsp90 ATPase inhibition by the Pih1-Tah1 complex, we propose that Pih1 anchored to the Hsp90 C domain through Tah1 also binds to the Hsp90 middle domain (M, *orange*) to lock the hinge (*red*) between Hsp90 M and C domains in an open conformation. This would preclude Hsp90 N domain dimerization and facilitate client binding.

ing of RNA moiety of RNPs during their assembly. Alternatively, the Hsp90-Tah1-Pih1 machinery could be necessary for the Rvb1/Rvb2 oligomeric association and/or dissociation during RNP maturation (44).

Acknowledgments—We thank Laurence H. Pearl (Institute of Cancer Research, London) for the plasmid pRSETA-hsp82. The protein expression tests and ultracentrifugation work have benefitted from the LEBS facilities of the IMAGIF Structural Biology and Proteomic of the Gif campus. We thank the Fondation pour la Recherche Médicale for a Synapt HDMS mass spectrometer.

REFERENCES

1. Wu, C. (1995) *Annu. Rev. Cell. Dev. Biol.* **11,** 441–469
2. De Maio, A. (1999) *Shock* **11,** 1–12
3. Houry, W. A. (2001) *Curr. Protein Pept. Sci.* **2,** 227–244
4. Young, J. C., Barral, J. M., and Ulrich Hartl, F. (2003) *Trends Biochem. Sci.* **28,** 541–547
5. Pearl, L. H., and Prodromou, C. (2001) *Adv. Protein Chem.* **59,** 157–186
6. Picard, D. (2002) *Cell. Mol. Life. Sci.* **59,** 1640–1648
7. Pratt, W. B., and Toft, D. O. (2003) *Exp. Biol. Med. (Maywood).* **228,** 111–133
8. Prodromou, C., and Pearl, L. H. (2003) *Curr. Cancer Drug. Targets.* **3,** 301–323
9. Pearl, L. H., and Prodromou, C. (2006) *Annu. Rev. Biochem.* **75,** 271–294
10. Prodromou, C., Panaretou, B., Chohan, S., Siligardi, G., O'Brien, R., Ladbury, J. E., Roe, S. M., Piper, P. W., and Pearl, L. H. (2000) *EMBO. J.* **19,** 4383–4392
11. Zhao, R., Davey, M., Hsu, Y. C., Kaplanek, P., Tong, A., Parsons, A. B., Krogan, N., Cagney, G., Mai, D., Greenblatt, J., Boone, C., Emili, A., and Houry, W. A. (2005) *Cell* **120,** 715–727
12. McClellan, A. J., Xia, Y., Deutschbauer, A. M., Davis, R. W., Gerstein, M., and Frydman, J. (2007) *Cell* **131,** 121–135
13. Millson, S. H., Truman, A. W., Wolfram, F., King, V., Panaretou, B., Prodromou, C., Pearl, L. H., and Piper, P. W. (2004) *Cell. Stress Chaperones.* **9,** 359–368
14. Zhao, R., Kakihara, Y., Gribun, A., Huen, J., Yang, G., Khanna, M., Costanzo, M., Brost, R. L., Boone, C., Hughes, T. R., Yip, C. M., and Houry, W. A. (2008) *J. Cell. Biol.* **180,** 563–578
15. Gonzales, F. A., Zanchin, N. I., Luz, J. S., and Oliveira, C. C. (2005) *J. Mol. Biol.* **346,** 437–455
16. Te, J., Jia, L., Rogers, J., Miller, A., and Hartson, S. D. (2007) *J. Proteome Res.* **6,** 1963–1973
17. Boulon, S., Marmier-Gourrier, N., Pradet-Balade, B., Wurth, L., Verheggen, C., Jády, B. E., Rothé, B., Pescia, C., Robert, M. C., Kiss, T., Bardoni, B., Krol, A., Branlant, C., Allmang, C., Bertrand, E., and Charpentier, B. (2008) *J. Cell. Biol.* **180,** 579–595
18. Millson, S. H., Vaughan, C. K., Zhai, C., Ali, M. M., Panaretou, B., Piper, P. W., Pearl, L. H., and Prodromou, C. (2008) *Biochem. J.* **413,** 261–268
19. Schmidt, T. G., and Skerra, A. (2007) *Nat. Protoc.* **2,** 1528–1535
20. Ali, M. M., Roe, S. M., Vaughan, C. K., Meyer, P., Panaretou, B., Piper, P. W., Prodromou, C., and Pearl, L. H. (2006) *Nature* **440,** 1013–1017
21. Shevchenko, A., Loboda, A., Ens, W., and Standing, K. G. (2000) *Anal. Chem.* **72,** 2132–2141
22. Schuck, P. (2000) *Biophys J.* **78,** 1606–1619
23. Wiseman, T., Williston, S., Brandts, J. F., and Lin, L. N. (1989) *Anal. Biochem.* **179,** 131–137
24. Sanglier, S., Atmanene, C., Chevreux, G., and Dorsselaer, A. V. (2008) *Methods Mol. Biol.* **484,** 217–243
25. Panaretou, B., Prodromou, C., Roe, S. M., O'Brien, R., Ladbury, J. E., Piper, P. W., and Pearl, L. H. (1998) *EMBO J.* **17,** 4829–4836
26. Zhao, R., Leung, E., Grüner, S., Schapira, M., and Houry, W. A. (2010) *PLoS One.* **5,** e9934
27. Sommer, N., Depping, R., Piotrowski, M., and Rüger, W. (2004) *Biochem. Biophys. Res. Commun.* **323,** 809–815
28. Cantor, C. R., and Schimmel, P. R. (1980) *Techniques for the Study of Biological Structure and Function*, W. H. Freeman
29. D'Andrea, L. D., and Regan, L. (2003) *Trends Biochem. Sci.* **28,** 655–662
30. Prodromou, C., Siligardi, G., O'Brien, R., Woolfson, D. N., Regan, L., Panaretou, B., Ladbury, J. E., Piper, P. W., and Pearl, L. H. (1999) *EMBO J.* **18,** 754–762
31. Siligardi, G., Panaretou, B., Meyer, P., Singh, S., Woolfson, D. N., Piper, P. W., Pearl, L. H., and Prodromou, C. (2002) *J. Biol. Chem.* **277,** 20151–20159
32. Meyer, P., Prodromou, C., Hu, B., Vaughan, C., Roe, S. M., Panaretou, B., Piper, P. W., and Pearl, L. H. (2003) *Mol. Cell.* **11,** 647–658
33. Cliff, M. J., Williams, M. A., Brooke-Smith, J., Barford, D., and Ladbury, J. E. (2005) *J. Mol. Biol.* **346,** 717–732
34. Ghaemmaghami, S., Huh, W. K., Bower, K., Howson, R. W., Belle, A., Dephoure, N., O'Shea, E. K., and Weissman, J. S. (2003) *Nature* **425,** 737–741
35. Retzlaff, M., Hagn, F., Mitschke, L., Hessling, M., Gugel, F., Kessler, H., Richter, K., and Buchner, J. (2010) *Mol. Cell.* **37,** 344–354
36. Young, J. C., and Hartl, F. U. (2000) *EMBO J.* **19,** 5930–5940
37. Panaretou, B., Siligardi, G., Meyer, P., Maloney, A., Sullivan, J. K., Singh, S., Millson, S. H., Clarke, P. A., Naaby-Hansen, S., Stein, R., Cramer, R., Mollapour, M., Workman, P., Piper, P. W., Pearl, L. H., and Prodromou, C. (2002) *Mol. Cell.* **10,** 1307–1318
38. Roe, S. M., Ali, M. M., Meyer, P., Vaughan, C. K., Panaretou, B., Piper, P. W., Prodromou, C., and Pearl, L. H. (2004) *Cell* **116,** 87–98
39. Richter, K., Muschler, P., Hainzl, O., Reinstein, J., and Buchner, J. (2003) *J. Biol. Chem.* **278,** 10328–10333
40. Onuoha, S. C., Coulstock, E. T., Grossmann, J. G., and Jackson, S. E. (2008) *J. Mol. Biol.* **379,** 732–744
41. Wegele, H., Haslbeck, M., Reinstein, J., and Buchner, J. (2003) *J. Biol. Chem.* **278,** 25970–25976
42. Granato, D. C., Gonzales, F. A., Luz, J. S., Cassiola, F., Machado-Santelli, G. M., and Oliveira, C. C. (2005) *FEBS J.* **272,** 4450–4463
43. Papin, C., Humbert, O., Kalashnikova, A., Eckert, K., Morera, S., Kas, E., and Grigoriev, M. (2010) *FEBS J.* **277,** 2705–2714
44. Niewiarowski, A., Bradley, A. S., Gor, J., McKay, A. R., Perkins, S. J., and Tsaneva, I. R. (2010) *Biochem. J.* **429,** 113–125
45. Geoghegan, K. F., Dixon, H. B., Rosner, P. J., Hoth, L. R., Lanzetti, A. J., Borzilleri, K. A., Marr, E. S., Pezzullo, L. H., Martin, L. B., LeMotte, P. K., McColl, A. S., Kamath, A. V., and Stroh, J. G. (1999) *Anal. Biochem.* **267,** 169–184